Asteroseismic Analysis of α Cen B: Preliminary Tests of Effects of Rotation and Interior Magnetic Field in the Solar-like Star [*]

Yan-Ke Tang[1,3], Shao-Lan Bi[2,1], Ning Gai[1,3] and Hua-Yin Xu[1]

[1] National Astronomical Observatories / Yunnan Observatory, Chinese Academy of Sciences, Kunming
650011, China; *tangyanke@ynao.ac.cn; bisl@bnu.edu.cn*
[2] Department of Astronomy Beijing Normal University, Beijing 100875, China
[3] Graduate School of Chinese Academy of Sciences, Beijing 100049, China

Abstract Taking into consideration the effects of rotation and interior magnetic field during the lifetime of the star, we reconstruct the model of α Cen B to satisfy the latest non-asteroseismic and asteroseismic observational constraints. We find that the effects can induce a change of about 0.3 μHz in the large frequency spacings and can speed up the star's evolution. The model of α Cen B has thereby been improved.

Key words: stars: oscillations — stars: interiors — stars: individual (α Cen B)

1 INTRODUCTION

The companion of α Cen A, α Cen B (HD 28621, HR 5460, Mv = 1.33), is a member of the α Cen AB binary system. The binary system is the closest system to the Earth (d = 1.34 pc) and has an eccentric orbit (e = 0.519) with a period of almost 80 years (Pourbaix et al. 2002). As a K-dwarf star, α Cen B has displayed the unambiguous signature of magnetic field in its observed spectrum (Char et al.1993; Rüedi et al. 1997; Robrade 2005). Thus, it is an important representative of solar-like stars and can provide us the most accurate information on the internal structure of stars.

Since 1978, many models of α Cen B have been presented (Flannery & Ayres 1978; Demarque et al. 1986; Noels et al. 1991; Edmonds et al. 1992; Neuforge 1993; Lydon et al. 1993; Fernandes & Neuforge 1995; Kim 1999; Pourbaix et al. 1999; Morel et al. 2000; Guenther & Demarque 2000). With advanced observational technique, Pourbaix et al. (2002) obtained a very precise mass of $0.934 \pm 0.061 M_\odot$ for α Cen B based on an accurate estimate of the parallax (Söderhjelm 1999) and new radial velocities. Recently, many p-mode oscillation frequencies of α Cen B were identified by many groups (Schou et al. 2001; Régulo et al. 2002; Carrier & Bourban 2003; Kjeldsen et al. 2005). The measurement of the frequencies of p-mode oscillation provides an insight into the internal structure of stars and provides the most powerful constraint on the theory of stellar evolution. Using the Geneva evolution code with atomic diffusion, Eggenberger et al. (2004) computed the model of α Cen B based on the seismological data obtained by Carrier & Bourban (2003). It is fortunate that 37 p-modes with $l = 0 - 3$ have been detected in α Cen B by Kjeldsen et al. (2005): these can be used to constrain further the theoretical model.

Magnetic field has been detected in stars located throughout the Hertzsprung-Russell diagram. Especially, the magnetic field and their related activities are ubiquitous among late-type stars with masses $M \leq 1 M_\odot$ (Landstreet 1992; Charbonneau et al. 2001), and the magnetic field accompanies the evolution of late-type stars. Eggenberger et al. (2006) proposed that shellular rotation can change the fundamental

stellar parameters and greatly increase the age of the star, and they suggested that a comprehensive treatment of rotation and magnetic field is needed. Brown et al. (1994) proposed that accurate oscillation data could provide a confrontation with the theory of stellar structure, thus involving phenomena that are not included in traditional treatments of stellar evolution. Now, stellar magnetic phenomena are related to stellar rotation: the evolution of the rotation rate is largely determined by the loss of angular momentum from magnetized stellar winds (Kawaler 1988; Weber & Davis 1967). Stellar rotation is found to correlate with chromospheric activity and other magnetic tracers (for a review see Hartmann & Noyes 1987). This is in favor of the idea that rotation plays a crucial role in the generation of stellar magnetic fields, through the operation of a dynamo.

In this paper, we check the effect of the magnetic field induced from rotation on the model of α Cen B based on the observational constraints, we examine the role of the effect on the interior of solar-like stars. In Section 2, we summarize in detail the observational results of α Cen B. In Section 3, we introduce Spruit's approach (Spruit 1999, 2002) and assume a distribution of magnetic field in the convection zone. The input physics and evolved models are given in Section 4. Then, in Section 5 the pulsation analysis is carried out. Finally, we present our results in Section 6.

2 OBSERVATIONS

2.1 Non-Asteroseismic Constraints

Using data from different sources, Pourbaix et al. (2002) improved the precision of the orbital parameters of α Cen and adopted the parallax derived by Söderhjelm (1999), $\varpi = 747.1 \pm 1.2$ mas. Finally, they determined a precise mass $0.934 \pm 0.0061 M_\odot$ for α Cen B, which we shall adopt in this work.

Some investigators (French & Powell 1971; Ayres et al. 1976) have investigated the abundance distribution in α Cen B using the differential curve-of-growth technique in moderately high dispersion spectrograms (2.4 Å mm^{-1}), and the results show that α Cen B is slightly metal-rich compared to the Sun, perhaps by as much as a factor of 2. Chmielewski et al. (1992) analyzed the iron abundance and obtained the final results [Fe/H]$_s$ = 0.26 ± 0.04. To deduce $[Z/X]_s$, we assumed $[Z/X]_s$ to be proportional to [Fe/H]$_s$ (Thoul et al. 2003; Eggenberger et al. 2005a) as follows:

$$\log[Z/X]_s \cong [\text{Fe/H}]_s + \log[Z/X]_\odot, \tag{1}$$

where $[Z/X]_\odot$ = 0.023 was given by Grevesse & Sauval (1998). Using this ratio, we adopt the $(Z/X)_s =$ 0.042 ± 0.003 as the model constraint.

For the effective temperature and luminosity, we took the mean values $T_{\text{eff}} = 5260 \pm 50$ K and $L/L_\odot =$ 0.503 ± 0.020, consistent with Eggenberger et al. (2004).

Kervella et al. (2003) measured the angular diameters of α Cen B using the VINCI instrument of the ESO's VLT interferometer. We used the radius of $0.863 \pm 0.005 R_\odot$ obtained by them to constrain our model.

Rotation velocity is vital to understand the magnetic behavior of stars. For the surface velocity of α Cen B, Char et al. (1993) found $P_{\text{rot}} = 43.3 \pm 1.5$ days based on the modulation of $C_{\alpha II}$ HK core emission; this is consistent with the period predicted from the flux and the Noyes relation. They obtained its equatorial velocity to be 1.02 ± 0.1 km s^{-1}.

We give a summary of the non-asteroseismic constraints in Table 1.

Table 1 Non-Asteroseismic Constraints

Parameters	α Cen B	References
$M_B/M_\odot$	0.934 ± 0.0061	Pourbaix et al. (2002)
T_{eff} (K)	5260 ± 50	Eggenberger et al. (2004)
$L/L_\odot$	0.503 ± 0.020	Eggenberger et al. (2004)
[Fe/H]$_s$	0.26 ± 0.04	Chmielewski et al. (1992)
$[Z/H]_s$	0.042 ± 0.003	this paper
$R/R_\odot$	0.863 ± 0.005	Kervella et al. (2003)
V_s (km s^{-1})	1.02 ± 0.1	Char et al. (1993)

2.2 Asteroseismic Constraints

Following the five-minute oscillations in the Sun which had led to a wealth of information about the solar interior, attempts have been made to detect a similar signal on other solar-like stars, and 12 oscillation modes were observed and identified by means of radial velocity measurements (Carrier & Bourban 2003). Subsequently, Kjeldsen et al. (2005) identified 37 oscillation modes with $l = 0 - 3$. The details of the oscillation frequency obtained by Kjeldsen et al. (2005) are summarized in Table 3, serving as asteroseismic constraints.

3 ABOUT THE ROTATION AND MAGNETIC FIELD

The generation of stellar magnetic field has remained a controversial issue so far. Some investigators thought that the magnetic field may be fossil field (Cowling 1945; Moss 1987; Braithwaite 2004), that is, a remnant from the star's formation. Other investigators preferred the field to be generated by a convective stellar dynamo (Parker 1979; Charbonneau & MacGregor 2001) in the convection zone or by the Tayler-Spruit dynamo (Pitts & Tayler 1985; Spruit 2002) in the differential rotational radiative region of the star. So far, the dynamo theory that the toroidal field is generated or stored at the bottom of the convection zone (Spiegel & Weiss 1980; Golub et al. 1981; Galloway & Weiss 1981; Choudhuri 1990; Brandenburg 2005b) is attractive, since there is a strong radial shear layer at that location, where $r\partial\Omega/\partial r \neq 0$.

In this paper, we use the Tayler-Spruit dynamo theory proposed by Spruit (2002). This dynamo is based on the Tayler instability that occurs in the radiative region (Tayler 1973; Pitts & Tayler 1985). Once a very weak horizontal magnetic field is subject to the Tayler instability, a vertical field component is created and is wound up by the differential rotation. As a result, the field lines become progressively closer and denser, so creating a strong horizontal field at the expense of the energy of the differential rotation (Eggenberger et al. 2005). In other words, a toroidal field is wound up by differential rotation from a week seed field. This mechanism has been applied to massive stars by researchers (Heger et al. 2003; Maeder & Meynet 2003, 2004, 2005; Mullan & MacDonald 2005). Here we apply it to the solar-like star α Cen B, to learn the magnetic effects induced in the Tayler-Spruit-dynamo theory on low-mass stars. Accordingly, for the radiative region of α Cen B, the magnetic field profile and strength are calculated by the Spruit formulate:

$$B_\varphi = r(4\pi\rho)^{1/2}\Omega \, q^{1/2}(\Omega/N)^{1/8}(\kappa/r^2N)^{1/8}, \tag{2}$$

and the equilibrium radial field is given by

$$B_r = B_\varphi(\omega/N)^{1/4}(\kappa/r^2N)^{1/4}. \tag{3}$$

In these two formulas, $q = \frac{\partial \ln \Omega}{\partial \ln r}$ is the dimensionless differential rotation rate, N is the Brunt-Väisälä (or buoyancy) frequency, and $\kappa = 16\sigma T^3/(3\kappa_R\rho^2 c_p)$ is the thermal diffusivity. There are no free parameters in Spruit's formula. Applying these formulas to the present Sun, Spruit (2002) obtained $B_\varphi \approx 1.5 \times 10^4$ G, $B_r \approx 1$ G (eq. (49)) and $\frac{B_r}{B_\varphi} \approx 10^{-5}$. We used this approximate relation of $B \sim B_\varphi$, when constructing the model of α Cen B. Figure 1a shows the angular velocity profile. Figure 1b shows the interior magnetic field strength induced by the differential rotation in the radiative region.

We assume that the magnetic field can be pumped from the radiative region to the convection zone according to the numerical simulations, and that the magnetic field in the convection zone has a Gaussian profile (eq. (4), Browning et al. 2006):

$$B(r, \sigma) = B_0 \exp\left[-\frac{1}{2}(r - r_{\text{cz}})^2/\sigma^2 \right], \tag{4}$$

where B_0 is the magnetic field at the bottom of the convection zone, at radius r_{cz}, and σ is an adjustable parameter (see the next section). Figure 1c shows the radial profile of the magnetic field strength in the convection zone.
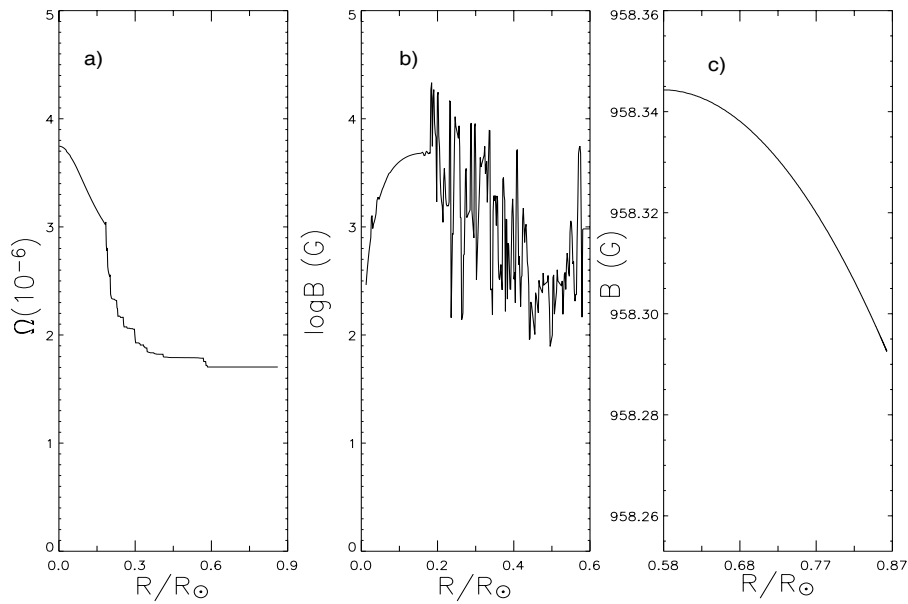
Fig. 1 Radial profiles of (a) angular velocity distribution, (b) logarithm of magnetic field strength in the radiative region, and (c) magnetic field strength in the convective region.

4 EVOLUTIONARY MODELS

Based on the work of Lydon & Sofia (1995) and Li & Sofia (2001), we modify the Yale Rotating Evolution Code (YREC) (Guenther et al. 1992) that computes stellar models including the rotation and interior magnetic field throughout the lifetime of the star. The magnetic field induced by rotation can impact on the stellar interior structure throughout the lifetime of α Cen B. See Appendixes A and B for the detailed description.

We ran the code from the initial zero-age main sequence (ZAMS). The models were computed using OPAL equation of state tables EOS2001 (Rogers & Nayfonov 2002), and the opacities interpolated between OPAL GN93 (Iglesias & Rogers 1996) and the low temperature tables (Alexander & Ferguson 1994). We used the standard mixing length theory to treat the energy transport in the convection zone and the nuclear reaction rates given by Bahcall & Pinsonneault (1995) to calculate the nuclear luminosity. We also considered the microscopic diffusion effect using the diffusion coefficients of Thoul et al. (1994). The Krishna-Swamy Atmosphere T-τ relation had been used in solar-like star by Guenther & Demarque (2000).

When considering the rotation and magnetic effects, we assumed solid body rotation imposed in the convective region, as was proposed by Pinsonneault et al. (1989). The initial angular velocity, a free parameter, can be adjusted until the surface velocity of the current model is near to the observed surface velocity. We adopted the Tayler-Spruit dynamo theory to produce the magnetic field in the radiative region only. Additional physical effects induced by rotation include: (a) effects on the structure of the star (Endal & Sofia 1976,1978); (b) loss of angular momentum due to magnetic wind (Kawaler 1988; Pinsonneault et al. 1989); (c) transport of angular momentum due to rotationally induced instabilities (Pinsonneault et al. 1989). We list the stellar structure equations modified by rotation in Appendix A, and the structure variables modified by magnetic field in Appendix B.

According to the results obtained by Eggenberger et al. (2004) and Miglio et al. (2005) on α Cen B, we adjusted the mass, mixing length parameters α and the initial chemical composition and computed a grid of evolved models so as to reproduce the observational constraints of α Cen B.

In this way, we obtain a grid of models along the evolutionary tracks with various sets of modeling parameters which satisfy all the non-asteroseismic observational constraints, i.e., the effective temperature, the luminosity, the radius and the surface metallicity, etc.

Table 2 Models of α Cen B. The left part gives the modeling input parameters, and the right part the global parameters of the two models.

Parameters	M1	M2	Parameters	M1	M2
$M_B(M_\odot)$	0.929	0.929	$L/L_\odot$	0.5025	0.4991
α	1.80	1.80	$T_{\text{eff}}(K)$	5220.27	5211.48
Z_0	0.034	0.034	$(Z/H)_s$	0.04332	0.04344
X_0	0.69	0.69	$R/R_\odot$	0.8689	0.8689
Ω_0	0	2.7×10^{-6}	$R_{\text{cz}}/R_\odot$	0.5856	0.5848
σ	0	22	V_s (km s^{-1})	0	1.03
			$\Omega_s(\times 10^{-6})$	0	1.703
			$t(\text{Gyr})$	5.970	5.856
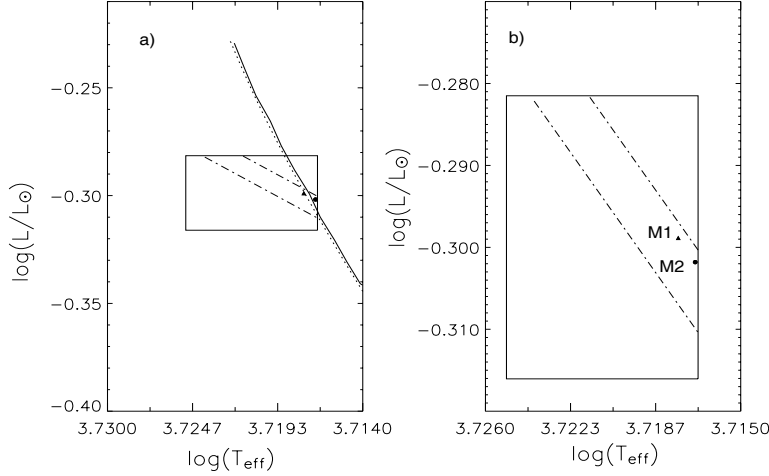
Fig. 2 a) Evolutionary tracks across the error boxes given by the observed luminosities and effective temperatures in the H-R diagram, the solid line and dotted line represent the model with and without rotation and magnetic effect using the same input physics, respectively. The dash-dotted lines denote the boxes delimited by the observed radii. b) A blow-up of the error box of panel a. The Models M1 and M2 are marked by the filled triangle and filled circle inside the error box, respectively.

For each stellar model of the grid so constructed, low-l p-mode frequencies are calculated using the *Guenther's* stellar pulsation code (Guenther 1994). In particular, the modes $l = 0 - 3$ were computed for the purpose of comparing with the observations.

Once the asteroseismic frequencies of all relevant models are computed, we use χ^2 minimization to deduce the set of parameters which leads to the best agreement with the observations. The result is the model M1 shown in Table 2 and Figure 2 as the ideal model without the rotation and magnetic field effects.

When we include the rotation and magnetic field effects, we only adjust the initial angular velocity and magnetic parameter σ, while the other input parameters are the same as for model M1. The magnitude of magnetic field in the radiative zone is given by Equation (2) and the profile of magnetic field in the convection zone is given by Equation (4) in which σ is adjusted to modify the profile. The surface velocity and other non-asteroseismic constraints of the models are compared with the observations. If the velocities of the models and the above non-asteroseismic constraints are not compatible with the observed values, the models are rejected and the procedure is repeated with another set of initial velocity and magnetic parameter σ. In this manner, we obtained the model M2 listed in Table 2 and Figure 2, which best agrees with the observations when we choose the initial angular velocity $\Omega_0 = 2.7 \times 10^{-6}$ and magnetic field parameter $\sigma = 22$ (cf. the broad Gaussian profile in Fig. 1c). It shows that the current surface velocity
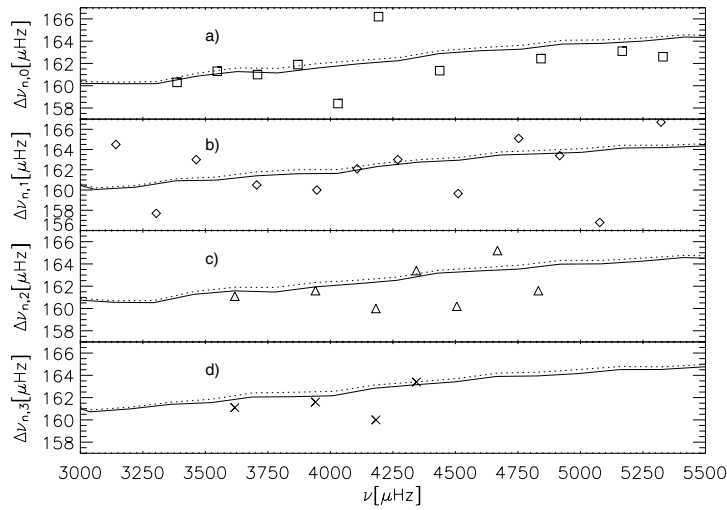
Fig. 3 Large spacing as function of the frequency for four values of l. The symbols (squares, diamonds, triangles, crosses) correspond to the observed values and that deduced from Kjeldsen et al. (2005), and the model values of model M1 and M2 are indicated by the dotted line and solid line, respectively.

deduced from the initial angular velocity is consistent with the observational values. The angular velocity distribution and the magnetic field profile have been shown in Figure 1.

For further investigation of the magnetic field effect, we list the detailed parameters of M1 and M2 in Table 2. The two models evolve up to the same radius using the same input parameters. Interestingly, we find that the age is less in model M2 than in model M1.

5 PULSATION ANALYSIS

Christensen-Dalsgaard (1986) proposed characterizing the stellar p-mode oscillation spectrum by two parameters: the large and the small spacings. With only two parameters to match, the task of comparing models with observed spectra is more easily quantified.

The large spacing $\Delta\nu$ and small spacing $\delta\nu_{nl}$ are defined as (Tassoul 1980):

$$\Delta\nu_{nl} \equiv \nu_{n,l} - \nu_{n-1,l}\,, \tag{5}$$

$$\delta\nu_{nl} \equiv \nu_{n,l} - \nu_{n-1,l+2}\,. \tag{6}$$

Comparing the theoretical large spacing and small spacing frequencies with the observational values, we select the model M2 as the best model for the case of including the rotation and magnetic field effects and the model M1 for the case of not including the effects. Both models evolve to the same radius $R \approx 0.868R_{\odot}$.

The asteroseismic features (the large spacings and the small spacings) are shown in Figures 3 and 4. From Figure 3 we find that the large spacing deduced from model M2 is closer to the observed value than that from model M1 and the difference between M1 and M2 is about 0.3 μHz. As regards the small spacings $\delta\nu_{02}$ and $\delta\nu_{13}$, we note that M2 is again better than model M1, see Figure 4.

We directly compare theoretical and observational frequencies, rather than their mean values over the large and small spacings. Figure 5 shows that the difference between the theoretical and observed values is less for the model M2 than for the model M1.

In order to compare more dramatically the theoretical p-model frequencies deduced from model M1 and M2 with the observed frequencies from Kjeldsen et al. (2005), we plot the echelle diagram of α Cen B. See Figure 6. We find that, on the whole, the observational frequencies are more consistent with the theoretical frequencies of M2 than with M1. It is shown that our model (model M2) is in good agreement with asteroseismic observations at low frequencies. The theoretical and observed frequencies are given in Table 3.
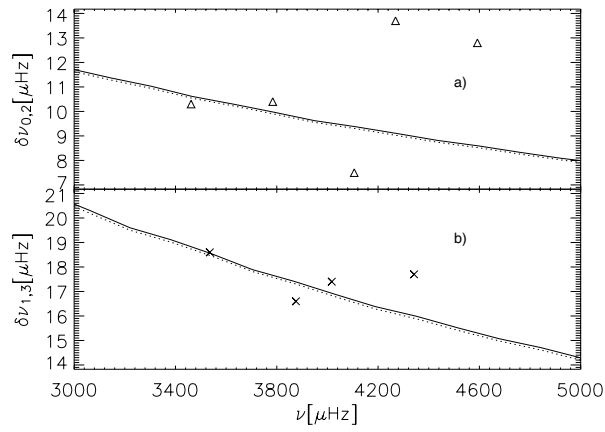
Fig. 4 Small spacings as function of the frequency for two values of l. The symbols and lines have the same meaning as in Fig. 3.
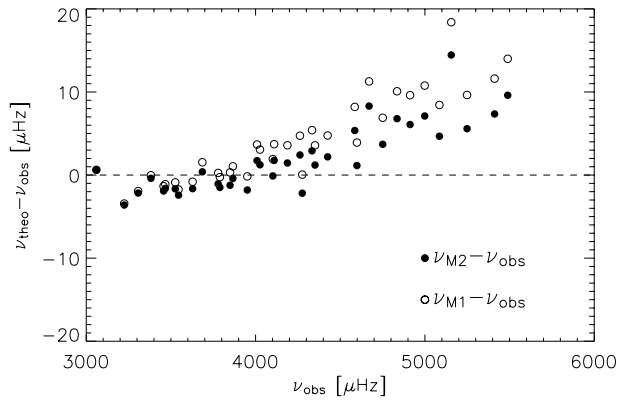
Fig. 5 Difference between theoretical and observed frequencies for Models M1 and M2. See also the separate plots of Figs. 3 and 4.
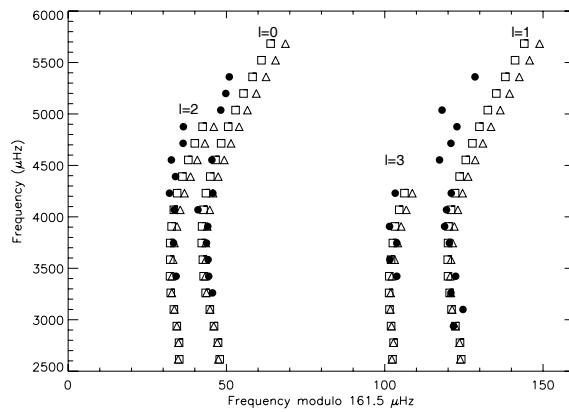
Fig. 6 Echelle diagram of α Cen B for the models M1 (open triangles) and M2 (open squares), for a large separation, $\Delta\nu = 161.5\,\mu$Hz. The filled circles correspond to the observed frequencies.

Table 3 Low degree p-mode frequencies (in μHz) for the model M2. The observations are obtained by Kjeldsen et al. (2005).

	Observations				Model M2			
n	$l = 0$	$l = 1$	$l = 2$	$l = 3$	$l = 0$	$l = 1$	$l = 2$	$l = 3$
17	...	3059.7	...	...	2984.073	3060.317	3132.883	3200.994
18	...	3224.2	...	...	3144.252	3220.593	3293.408	3362.391
19	3306.6	3381.9	3456.6	3526.3	3304.436	3381.506	3454.680	3523.942
20	3466.9	3544.9	...	3685.6	3465.294	3542.482	3616.262	3685.992
21	3628.2	...	3778.8	3849.3	3626.564	3703.886	3777.739	3848.071
22	3789.2	3865.9	...	4008.5	3787.710	3865.494	3939.678	4010.238
23	3951.1	4025.9	4102.0	...	3949.301	4027.132	4101.891	4173.070
24	4109.5	4188.0	4262.0	4333.3	4111.267	4189.453	4264.418	4336.217
25	4275.7	4351.0	4425.4	...	4273.517	4352.204	4427.591	4499.634
26	...	...	4585.6	...	4436.405	4515.148	4590.960	4663.533
27	4598.4	4670.3	4750.8	...	4599.548	4678.603	4754.501	4827.478
28	...	4835.4	4912.4	...	4762.827	4842.187	4918.480	4991.633
29	...	4998.8	...	...	4926.562	5005.909	5082.486	5156.144
30	5085.7	5155.6	...	...	5090.369	5170.051	5246.734	5320.668
31	5248.8	...	...	...	5254.384	5334.243	5411.306	5485.416
32	5411.4	5489.0	...	...	5418.755	5498.603	5575.797	5650.297

Table 4 Comparison of Models

Source	$M/M_\odot$	$\alpha = l/H_p$	Z_0	$(Z/X)_i$	Y_0	$R/R_\odot$	Age (Gyr)	Fitting Seismic Source
Eggenberger (2004)	0.934	1.97 ± 0.10	...	0.0434 ± 0.0020	0.275 ± 0.0010	0.870	6.52 ± 0.30	Carrier & Bourban (2003)
Miglio (2005)	0.934	2.61	0.0340	...	0.259	0.863	8.9	No Seismo
This paper	0.929	1.80	0.0340	...	0.276	0.8689	5.856	Kjeldsen et al. (2005)

Finally, we compare our model M2 with the results obtained by Eggenberger et al. (2004) and Miglio et al. (2005), see Table 4. We argue that our model is in better agreement with the observed radius than Eggenberger et al. (2004). In addition, the age of our model is lower than in the other models.

6 CONCLUSIONS

Rotation and magnetic field in the stellar interior will change the hydrostatic equilibrium and thermodynamic variables, and so will have a significant impact on stellar models. In particular, the oscillation frequencies are affected, and the change in the large spacings can be as much as about 0.3μHz. This is because the frequencies of these oscillation depend on the sound speed inside the star, which in turn depends on the density, temperature, gas motion, and other properties of the stellar interior. After taking into account the rotation and magnetic field effects, we find that the theoretical frequencies agree better with the observed values.

We summarize our work in this paper as follows:

1. We have reconstructed the model of α Cen B to include the rotation and interior magnetic field effects and the model has thereby been improved.
2. By comparing the model M1 with the model M2, we find that the effects of rotation and magnetic field can induce a change of about $0.3\,\mu$Hz in the large frequency spacings and speed up the star's evolution. The change can certainly be determined by the rotation velocity, and the magnitude and profile of the magnetic field. Our paper provides a preliminary test of the effects.
3. By reproducing the observed non-asteroseismic and asteroseismic constraints, we can estimate the intensity of the magnetic field in the star's interior. For the α Cen B we estimate that the magnetic field can be up to hundreds Gaussian in the convection zone (see Fig. 1c). If we have sufficient and precise

observed asteroseismic frequencies, we can further refine the estimate the interior magnetic field using the asteroseismic constraints.

4. Although our model including rotation and magnetic field effects can fit the non-asteroseismic and new asteroseismic observational data, further investigations of the geometry and precise strength of the magnetic field in the stellar interior are necessary and possible in future with the accumulation and improvement of observation data.

5. Eggenberger (2006) has shown that the lifetimes of the rotating models are increased, because mixing feeds the core with fresh hydrogen fuel, so increasing the time the star spends on the main sequence. Our result shows that, on the other hand, the rotation and magnetic effects can speed up the evolution.

Appendix A: ROTATING MODEL OF SOLAR-LIKE STARS

To construct model for a rotating star, we have to take into account two effects of rotation: centrifugal force and meridian circulation.

Centrifugal force can change the structure of a star from one of spherical symmetry to one of non-spherical symmetry. How to simplify the two-dimensional model with conservative rotation to a one-dimensional model? Several authors (Kippenhahn & Thomas 1970; Endal & Sofia 1976; Pinsonneault et al. 1989, 1990, 1991; Chaboyer et al. 1995a, 1995b; Langer 1998; Heger & Langer 1998; Meynet & Maeder 1997; Maeder & Meynet 2000; Huang 2004a, 2004b) have investigated this problem. In this paper we apply the YREC approach (Guenther et al. 1992) to construct models of the solar-like stars. The stellar model for rotating stars is based on the method developed by Kippenhahn & Thomas (1970) and modified by Endal & Sofia (1976, 1978). The mass continuity equation (Eq. (A.1)) is not varied with rotation, while the energy conservation equation (Eq. (A.3)) retains its nonrotating form. All the structural effects of rotation are limited with the equation of hydrostatic equilibrium (Eq. (A.2)) and the radiative temperature gradient(Eq. (A.4)). The modified structure equations are as follows:

$$\frac{\partial r}{\partial M_\psi} = \frac{1}{4\pi r_\psi^2 \rho_0}, \tag{A.1}$$

$$\frac{\partial P_0}{\partial M_\psi} = -\frac{GM_\psi}{4\pi r_\psi^4} f_p, \tag{A.2}$$

$$\frac{\partial L_\psi}{\partial M_\psi} = \varepsilon_n - \varepsilon_\nu - T\frac{dS_0}{dt}, \tag{A.3}$$

$$\frac{\partial T}{\partial M_\psi} = \Big[-\frac{GM_\psi T}{4\pi r_\psi^4 P_0} f_p\Big] \cdot \min\Big[\nabla_0, \frac{3\kappa_0 L_\psi P_0}{16\pi ac M_\psi T^4} \frac{f_T}{f_p}\Big], \tag{A.4}$$

where the nondimensional rotating corrective factors f_P and f_T depend on the shape of the isobars,

$$f_p = \frac{4\pi r_\psi^4}{GM_\psi S_\psi} \frac{1}{\langle g^{-1}\rangle}, \tag{A.5}$$

$$f_T = \Big(\frac{4\pi r_\psi^2}{S_\psi}\Big)^2 \frac{1}{\langle g\rangle\langle g^{-1}\rangle}. \tag{A.6}$$

Here $\langle g\rangle$, $\langle g^{-1}\rangle$ are the mean values of the effective gravity and its inverse over the equipotential surface. The equipotential surface is defined by

$$\psi = \frac{GM_\psi}{r} + \frac{1}{2}\omega^2 r^2 \sin^2\theta - \frac{4\pi}{3r^3}P_2(\cos\theta)\int_0^{r_0}\frac{\rho r_0'^6}{M_\psi}\omega^2\frac{5+\eta_2}{2+\eta_2}dr_0' = \text{constant}, \tag{A.7}$$

where S_ψ is the surface area of the equipotential, ∇_0 in Equation (A.4) is the convective temperature gradient.

Meridian circulation is quite a complicated issue, which can result in the transport of angular momentum and the chemical composition of a star. The effects have also been studied (Endal & Sofia 1976; Tassoul 1978; Schatzman et al. 1981; Langer 1991, 1992; Chaboyer & Zahn 1992; Zahn 1992; Heger et al. 2000; Maeder & Meynet 2000). Additionally, angular momentum loss is a ubiquitous feature in the early evolution of low-mass stars based on suggestions from the observations. Therefore, we must modify the total angular momentum to allow for this angular momentum loss from the surface when we advance the models. In this paper we used a more general parameterization (Kawaler 1988)

$$\frac{dJ}{dt} = -K_W \Omega^{1+(4an/3)} \Big(\frac{R}{R_\odot}\Big)^{2-n} \Big(\frac{\dot{M}}{10^{-14}}\Big)^{1-(2n/3)} \Big(\frac{M}{M_\odot}\Big)^{-n/3}. \tag{A.8}$$

The angular momentum and composition redistribution were computed using the coupled nonlinear diffusion equations (Pinsonneault et al. 1989):

$$\rho r^2 \frac{I}{M} \frac{d\omega}{dt} = f_\omega \frac{d}{dr}\Big(\rho r^2 \frac{I}{M} D \frac{d\omega}{dr}\Big), \tag{A.9}$$

and

$$\rho r^2 \frac{dX_i}{dt} = f_c f_\omega \frac{d}{dr}\Big(\rho r^2 D \frac{dX_i}{dr}\Big), \tag{A.10}$$

where D is the diffusion coefficient, f_c and f_ω are adjustable parameters.

Appendix B: MODIFIED STELLAR STRUCTURE EQUATIONS AND EQUATION OF STATE INCLUDING MAGNETIC FIELD

Lydon & Sofia (1995), Li & Sofia (2001), Bi et al. (2003), Liao & Bi (2004), Bi & Yan (2005) and Li et al. (2006) have studied the effect of magnetic field on the stellar structure equations. In this paper we concentrated on the modified structure variables by large scale magnetic field, $\boldsymbol{B} = (B_t, B_p)$. So, we introduce two magnetic structure variables since the magnetic field is a vector: the magnetic energy density χ (Lydon & Sofia 1995) and the ratio of specific heats for the magnetic perturbation γ (Lydon & Sofia 1995; Li & Sofia 2001):

$$\chi = (B^2/8\pi)/\rho, \tag{B.1}$$

$$\gamma = (2B_t^2 + B_p^2)/B^2, \tag{B.2}$$

where $B = (B_t^2 + B_p^2)^{1/2}$, B_t and B_p are the azimuthal and radial components of field, respectively. The magnetic pressure P_χ can be expressed as $P_\chi = (\gamma - 1)\chi\rho$. Therefore, the equations of stellar structure can be renewed as following:

$$\frac{\partial r}{\partial M_\psi} = \frac{1}{4\pi r_\psi^2 \rho}, \tag{B.3}$$

$$\frac{\partial P}{\partial M_\psi} = -\frac{GM_\psi}{4\pi r_\psi^4} f_p, \tag{B.4}$$

$$\frac{\partial L_\psi}{\partial M_\psi} = \varepsilon_n - \varepsilon_\nu - T\frac{dS}{dt}, \tag{B.5}$$

$$\frac{\partial T}{\partial M_\psi} = \Big[-\frac{GM_\psi T}{4\pi r_\psi^4 P}.f_p\Big] \cdot \min\Big[\nabla, -\frac{3\kappa L_\psi P}{16\pi ac M_\psi T^4}\frac{f_T}{f_p}\Big], \tag{B.6}$$

where

$$\rho = \rho_0 / \Big[1 + \frac{(\gamma - 1)\chi\rho_0}{P}\Big], \tag{B.7}$$

$$P = P_0 + (\gamma - 1)\chi\rho, \tag{B.8}$$

$$TdS = TdS_0 + d\chi, \tag{B.9}$$

$$\kappa = \kappa_0 - \kappa_e \frac{(\gamma - 1)\tau_e^2 \Omega_e^2}{4 + (\gamma - 1)\tau_e^2 \Omega_e^2}, \tag{B.10}$$

$$\nabla = (\partial \ln T / \partial \ln P_T)_s. \tag{B.11}$$

Then the equation of state becomes (Li & Sofia 2001):

$$\frac{d\rho}{\rho} = \alpha \frac{dP_T}{P_T} - \delta \frac{dT}{T} - \nu \frac{d\chi}{\chi} - \nu' \frac{d\gamma}{\gamma}, \tag{B.12}$$

where P_T is the total pressure, $\alpha = (\frac{\partial \ln \rho}{\partial \ln P_T})_{T,\chi,\gamma}$, $\delta = -(\frac{\partial \ln \rho}{\partial \ln T})_{P_T,\chi,\gamma}$, $\nu = -(\frac{\partial ln\rho}{\partial ln\chi})_{P_T,T,\gamma}$, and $\nu' = -(\frac{\partial \ln \rho}{\partial \ln \gamma})_{P_T,T,\chi}$.

References

Alexander D. R., Ferguson J. W., 1994, ApJ, 437, 879

Ayres T. R., Linsky J. L., Rodgers A. W. et al., 1976, ApJ, 210, 199

Bahcall J. N., Pinsonneault M. H., Wasserburg G. J., 1995, RvMP, 67, 781

Brandenburg A., 2005, eprint arXiv:astro-ph/0512637

Brown T. M., Christensen-Dalsgaard J., Weibel-Mihalas B. et al., 1994, ApJ, 427, 1013

Browning M. K., Miesch M. S., Brun A. S. et al., 2006, ApJ, 648, 157

Bi S. L., Liao Y., Wang J. X., 2003, A&A, 397, 1069

Bi S. L., Yan X. Y., 2005, A&A, 431, 1089

Bigot L., Kervella P., Thvenin F. et al., 2006, A&A, 446, 635

Carrier F., Bourban G., 2003, A&A, 406, 23

Char S., Foing B. H., Beckman J. et al., 1993, A&A, 276, 78

Charbonneau P., MacGregor K. B., 2001, ApJ, 559, 1094

Charboyer B., Zahn J. P., 1992, A&A, 253, 173

Charboyer B., Demarque P., Pinsonneault M. H., 1995a, ApJ, 441, 865

Charboyer B., Demarque P., Pinsonneault M. H., 1995b, ApJ, 441, 876

Chmielewski Y., Friel E. et al., 1992, A&A, 263, 219

Choudhuri A. R., 1990, ApJ, 355, 733

Christensen-Dalsgaard J., 1986, in: Seismology of the sun and the distant stars; Proceedings of the NATO Advanced
    Research Workshop, Cambridge, England, June 17-21, 1985 (A87-20101 07-92). Dordrecht: Reidel, p. 23

Cowling T. G., 1945, MNRAS, 105, 166

Demarque P., Guenther D. B., van Altena W. F., 1986, ApJ, 300, 773

Edmonds P., Cram L., Demarque P. et al., 1992, ApJ, 394, 313

Eggenberger P., Carrier F., Bouchy F., 2005a, NewA, 10, 315

Eggenberger P., Carrier F., Maeder A. et al., 2006, MmSAI, 77, 309

Eggenberger P., Maeder A., Meynet G., 2005b, A&A, 440, 9

Eggenberger P., Charbonnel C., Talon S. et al., 2004, A&A, 417, 235

Endal A. S., Sofia S., 1976, ApJ, 210, 184

Endal A. S., Sofia S., 1978, ApJ, 220, 279

Fernandes J., Neuforge C., 1995, A&A, 295, 678

French V. A., Powell A. L. T., 1971, R. Obser. Bull., 173, 63

Flannery B. P., Ayres T. R., 1978, ApJ, 221, 175

Galloway D., Weiss N. O., 1981, Geophys. Astrophys. Fluid Dyn., 243, 945

Golub L., Rosner R., Vaiana G. S. et al., 1981, ApJ, 243, 309

Grevesse N., Sauval A. J., 1998, Space Sci. Rev., 85, 161

Guenther D. B. et al., 1992, ApJ, 387, 372

Guenther D. B., 1994, ApJ, 422, 400

Guenther D. B., Demarque P., 2000, ApJ, 531, 503

Hartmann L. W., Noyes R. W., 1987, ARA&A, 25, 271

Heger A., Langer N., 1998, A&A, 334, 210

Heger A., Langer N., Woosley S. E., 2000, ApJ, 528, 368

Heger A., Woosley S. E., Langer N., 2003, IAUS212, edited by Karel van der Hucht, Artemio Herrero, Esteban, Csar.
     San Francisco: Astronomical Society of the Pacific, p.357
Huang R. Q., 2004a, A&A, 422, 981
Huang R. Q., 2004b, A&A, 425, 591
Iglesias C. A., Rogers F. J., 1996, ApJ, 464, 943
Kawaler S. D., 1988, ApJ, 333, 236
Kim Yong-Cheol, 1999, JKAS, 32, 119
Kippenhahn R., Thomas H. C., 1970, in: Stellar Rotation, ed. A. Slettebak, Dordrecht: Reidel, p. 20
Kervella P., Thévenin F., Ségransan D. et al., 2003, A&A, 404, 1087
Kjeldsen H., Bedding T. R., Butler R. P. et al., 2005, ApJ, 635, 1281
Landstreet J. D., 1992, A&A Rev., 4, 35
Langer N., 1991, A&A, 243, 155
Langer N., 1992, A&A, 265, L17
Langer N., 1998, A&A, 329, 551
Li L.H., Sofia S., 2001, ApJ, 549, 1204
Li L. H., Ventura P., Basu S. et al., 2006, ApJ, 164, 215
Liao Y., Bi S. L., 2004, Chin. J. Astron. Astrophys. (ChJAA), 4, 490
Lydon T. J., Fox P. A., Sofia, S., 1993, ApJ, 413, 390
Lydon T. J., Sofia S., 1995, ApJS, 101, 357
Maeder A., Meynet G., 2000, ARA&A, 38, 43
Maeder A., Meynet G., 2003, A&A, 411, 543
Maeder A., Meynet G., 2004, A&A, 422, 225
Maeder A., Meynet G., 2005, A&A, 440, 1041
Meynet G., Maeder A., 1997, A&A, 321, 465
Miglio A., Montalbán J., 2005, A&A, 441, 615
Morel P., Provost J., Lebreton Y. et al., 2000, A&A, 363, 675
Moss D., 1987, MNRAS, 226, 297
Mullan D. J., MacDonald, James , 2005, MNRAS, 356, 1139
Neuforge C., 1993, A&A, 268, 650
Noels A., Grevesse N., Magain P. et al., 1991, A&A, 247, 91
Parker E. N., 1979, in: Cosmical magnenic field: Their origin and their activity, Oxford: Clarendon Press, p.858
Pinsonneault M. H., Kawaler S. D., Sofia S. et al., 1989, ApJ, 338, 424
Pinsonneault M. H., Kawaler S. D., Demarque P., 1990, ApJ, ApJS, 74, 501
Pinsonneault M. H., Deliyannis C. P., , Demarque P., 1991, ApJ, 367, 239
Pitts E., Tayler R. J., 1985, MNRAS, 216, 139
Pourbaix D., Neuforge-Verheecke C., Noels A., 1999, A&A, 344, 172
Pourbaix D. et al., 2002, A&A, 386, 280
Régulo C., Cortés Roca. T., 2002, In: Proceedings of the First Eddington Workshop on Stellar Structure and Habitable
     Planet Finding, 11 - 15 June 2001, Crdoba, Spain. Editor: B. Battrick, Scientific editors: F. Favata, I. W. Roxburgh
     & D. Galadi. ESA SP-485, Noordwijk: ESA Publications Division, ISBN 92-9092-781-X, 2002, p.313
Rüedi I., Solanki S. K., Mathys G. et al., 1997, A&A, 318, 429
Robrade, J., Schmitt, J. H. M. M., Favata, F., 2005, A & A, 442, 315
Rogers F. J., Nayfonov A., 2002, ApJ, 576, 1064
Schatzman E., Maeder A., Agrand F. et al., 1981, A&A, 96, 1
Schou J., Buzasi D. L., 2001, ESASP, 464, 391
Spruit H. C., 1999, A&A, 349, 189
Spruit H. C., 2002, A&A, 381, 923
Spiegel E. A., Weiss N. O., 1980, Nature, 287, 616
Söderhjelm S., 1999, A&A, 341, 121
Tassoul J. L., 1978, in: Theory of Rotating Stars, Princeton: Princeton Univ. Press
Tassoul M., 1980, ApJS, 43, 469
Tayler R. J., 1973, MNRAS, 161, 365
Thoul A., Bahcall J. N., Loeb A., 1994, ApJ, 421, 828
Thoul A., Scuflaire R., Noels A. et al., 2003, A&A, 402, 293
Weber E. J., Davis L. J., 1967, ApJ, 148, 217
Zahn J.-P., 1992, A&A, 265, 115